SYNTHETIC FOCUSING FOR IMAGING THE ULTRASONIC BACKSCATTERED NOISE IN DUAL PHASE TITANIUM FORGED PARTS

C. Bescond, D. Lévesque, J.-B. Guénette and J.-P. Monchalin
Industrial Materials Institute, National Research Council Canada, Boucherville, Quebec, Canada

Abstract: The inspection of titanium billets and forged parts with conventional immersion and laser-ultrasonic techniques was performed to localize macro-zones with strong texture. The microtextured regions in these dual phase titanium parts were detected by using backscattered noise measurements. A numerical focusing technique was developed for imaging the backscattered noise in parts with curved surfaces. This technique allows controlling the focusing of the ultrasonic beam to improve the contrast of backscattered noise images.

Introduction: The ultrasonic inspection is the prime candidate for bulk non-destructive micro-structural characterization of two-phase titanium-forged parts. Backscattered signal has been widely used to control or characterize two-phase titanium billets [1-4]. The two-phase titanium billet is formed of small grains grouped together within former large beta grains [5]. The small grains within a former large beta grain have very close crystallographic orientation. The "highly microtextured regions", called "macrograins", form macrostructures that influence greatly the elastic properties of the titanium-forged parts. The backscattered noise observed in this material should be sensitive to the shape and orientation of the macrograins.

In this work, a procedure based on the SAFT (Synthetic Aperture Focusing Technique) is developed to map the backscattered noise. One advantage of this technique is the capability to control numerically the aperture of the acoustic beam. As a result, the acoustic beam can be focused at different depths inside the sample with the desired aperture. Note that, in the case of physical focusing and due to the refraction in titanium, a large acoustical beam aperture would require a focused transducer with a very large diameter.

The results obtained clearly show noise bands in the titanium billet that originate from the thermo-mechanical processing. In the forged material, different high noise regions are detected and correlations of these regions with the flow lines are found. Noise regions with angular dependence that could be associated with the original micro-texture of the billet are also reported.

Immersion technique: The immersion set up used for measurements is illustrated in Figure 1. The titanium billet is positioned onto a rotating table and the transducer is mounted on an arm that possesses degrees of freedom in translations and rotations to perform scans or adjustments. Line focused and unfocused transducers with 10 MHz center frequency are used in the measurements.

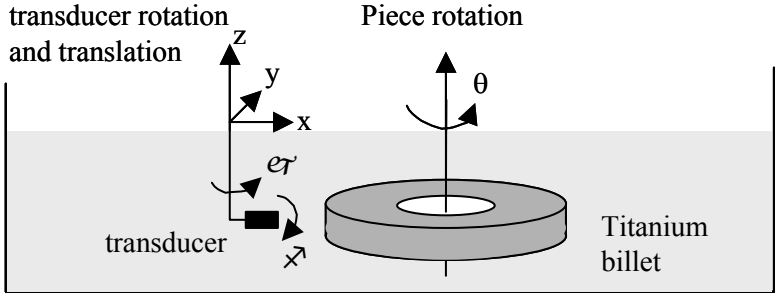

Figure 1. Immersion set up.

In this work, the measurements are performed in the radial direction for which the interaction between the acoustic waves and the macrograins should be stronger. The scans are performed by imposing a rotation of the table, therefore scanning the angle θ in Figure 1. In Figure 2, the image of the backscattered noise for radial propagation obtained with an unfocused transducer reveals high and low noise bands located at different angular positions. In this figure, the backscattered noise is mapped onto the disc-shape of the billet and typical signals obtained in the low and high-noise bands are shown. In these waveforms, the front echo that propagates only into water arrives at time 0 and the back wall echo arrives at a time around 14.5 μs. The discontinuities between these two echoes correspond to the backscattered noise due to the interaction of the incident acoustic beam with the microstructure of the dual phase titanium alloy.

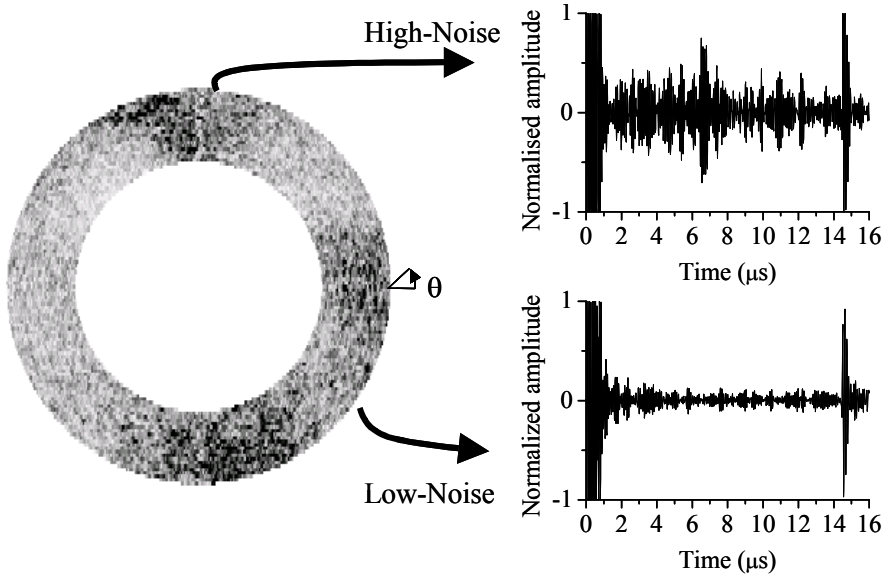

Figure 2. RMS value of the backscattered noise mapped onto the disc-shape of the billet using an unfocused transducer and typical acoustic waveforms in the low and high-noise bands.

As mentioned, the dual phase titanium alloy has small grains grouped within macrograins with a strong texture related to that of the former large beta grains. Notice that the micro-texture in the macrograin is complex since there are primary alpha, secondary alpha and beta colonies with different crystallographic orientations that satisfy the Bürger's relationships. Current theories suggest that the feature that controls the backscattered noise is the two-point correlation of the elastic constants [3, 6], and relates to local variations in the crystallographic orientation. The backscattered noise level depends simultaneously on the micro-texture of the macrograins and on their shapes and orientations. In particular, the backscattered noise is highly affected by the effective boundary of the macrograins viewed by the incident acoustic beam, also called scattering cross-section. Notice that the microstructure of individual alpha and beta grains cannot be the source of the backscattered noise since their size of typically 10 μm is much less than the acoustic wavelength of 600 μm at 10 MHz. It is therefore the macrograins with a size of typically 1 mm that control the noise generation in the duplex titanium alloy.

The microtextured regions in the billet have columnar shapes elongated along the axial direction (z-axis in Fig. 1) due to a reduction in diameter. Related to the scattering cross-section, a low backscattered noise level is observed for incident acoustic waves along the z-axis of the billet while a higher backscattered noise level with strong bands are observed for waves along the radial direction. During the thermo-mechanical processing, in addition to the elongation of the

prior beta grain in the axial direction, a secondary elongation occurs, which is dominant in either the radial (r-axis) or the hoop (angle θ) direction, when the billet is forged from a square cross-section to a circular cross-section. As a result, high and low-noise regions are observed since the scattering cross-section may change with angular position depending on the orientation of the macrograins. This also explains the symmetry observed in the presence of high-noise bands separated by 90º, going from a square billet to a cylindrical one.

SAFT processing: To enhance backscattered noise signal and spatial resolution, focused transducers are usually used to concentrate the acoustic beam at different locations into the material. To map the backscattered noise, the focal point position of the transducer is scanned in the bulk of the piece. Due to refraction in the titanium, a large aperture of the acoustical beam would require a focused transducer with a very large diameter. In this work, a procedure based on the SAFT (Synthetic Aperture Focusing Technique) [7, 8] is developed to improve imaging of the backscattered noise. One advantage of SAFT is the capability to control numerically the aperture of the acoustic beam. As a result, the acoustic beam can be focused at different locations inside the sample with the desired aperture. Note that the technique developed in this work for imaging backscattered noise differs from the usual SAFT processing. The summation is not performed on the time signal, since in fact, this would be equivalent to spatial averaging and would cancel out the backscattered noise signal from the microstructure. The summation is rather performed on the signal squared, relating to energy, and the RMS value of the result is then displayed as SAFT image. Moreover, the SAFT reconstruction takes into account the curvature of the part to be inspected from the inner or the outer surface.

In Figure 3a, the principle of the synthetic aperture focusing is illustrated. The arrows represent different diverging sources onto the surface from which A-scan signals are measured. For a given focal point to probe, the energy of all signals within the desired angular aperture are shifted in time and summed together. In the figure, the angular aperture is defined as β_{max} and the gray arrows correspond to the diverging sources that contribute to the point M. With respect to the geometric constructions in Figs. 3b and 3c, the expression for the path, p, used for time shifting is:

$$p^2 = r^2 + (r - x)^2 - 2r(r - x)\cos(\beta - \alpha) \quad \text{with } \sin\alpha = \frac{r - x}{r}\sin\beta, \quad \beta \le \beta_{max} \tag{1}$$

for the outer surface, and

$$p^2 = r^2 + (r + x)^2 - 2r(r + x)\cos(\beta - \alpha) \quad \text{with } \sin\alpha = \frac{r + x}{r}\sin\beta, \quad \beta \le \beta_{max} \tag{2}$$

for the inner surface. In the equations and figures, r is the radius of the curved surface.

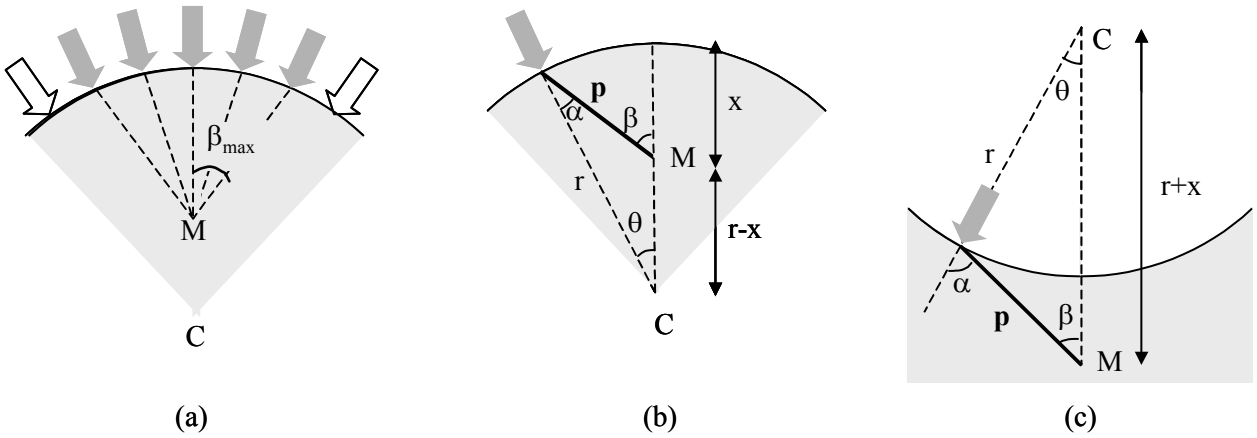

Figure 3. (a) Principle of SAFT with a curved surface; reconstruction for an outer surface (b) and an inner surface (c).

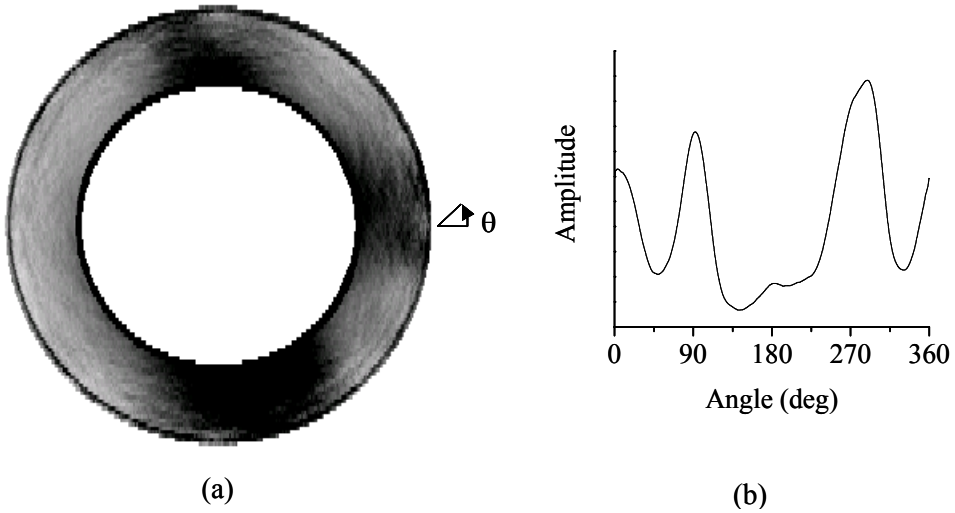

Figure 4. (a) SAFT image of the RMS value of the backscattered noise obtained with a 1-in line focused transducer; (b) angular dependence of the RMS value averaged along the radial direction.

The actual angular aperture available for SAFT processing is controlled by the divergence of the acoustical beam in the medium. A 1-in line focused transducer positioned at 1 inch from the titanium billet has been used to perform a circular scan (angle θ) and SAFT processing of the backscattered noise. For the reconstruction, a 20 deg aperture has been considered. With a line source onto the sample surface along the z-axis, the divergence into the sample is important in the plane x-y (see Figs. 1 and 3). Figure 4a shows the SAFT image of the RMS value of the backscattered noise obtained for the titanium billet. In Figure 4b, the angular dependence of the RMS value averaged along the radial direction after SAFT processing is shown. In these figures, three high noise bands are clearly observed and a fourth band smaller than the others appears near 180 deg. Comparing Figs. 2 and 4, the SAFT processing provides images of noise bands with more contrast than conventional B-scans. Also, no additional structure in the backscattered noise is observed with SAFT processing. For a forged titanium part, the improvement with SAFT processing should be more prominent since the macrograins have more complex orientations following the forging flow lines.

Laser-ultrasonic technique: Measurements have also been performed with the laser ultrasonic set up shown in Figure 5. Laser-ultrasonics [9, 10] uses two lasers, one with a short pulse for the generation of ultrasound and another one, long pulse or continuous, coupled to an optical interferometer for detection. Laser-ultrasonics is a technique that combines the advantages of both optical and ultrasonic sensing. Laser-ultrasonics allows sensing remotely as an optical technique and sensing inside materials as well as on their surface as an ultrasonic technique. The technique features also a large detection bandwidth, which is particularly important for material characterization. Another feature of laser-ultrasonics, particularly useful for testing parts of complex shapes, is the generation of an ultrasound wave propagating at well-defined angles, independently of the shape of the part and of the incidence angle of the optical generation beam. A pulsed Nd: YAG laser (3rd harmonic: 355 nm wavelength, 8 ns pulse duration) is used to generate acoustic waves in the ablation regime. For the detection, a pulsed Nd: YAG laser (1064 nm; 200 μs pulse duration) is coupled to a confocal Fabry-Perot interferometer by optical fibers to measure the acoustic surface displacement. A rotating table is used to perform scanning of the billet.

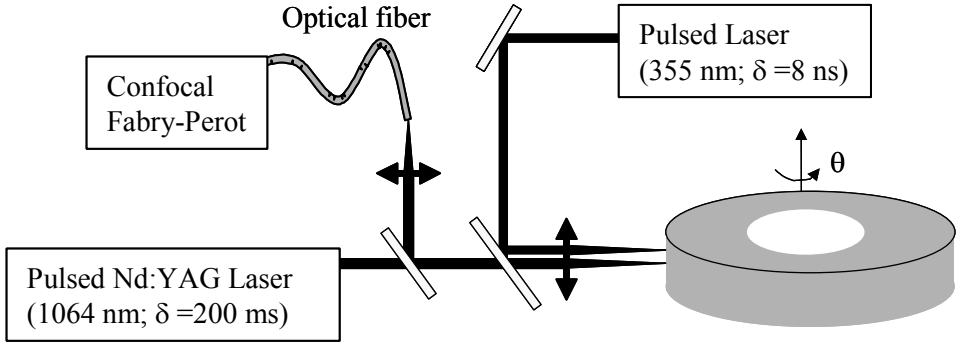

Figure 5. Laser ultrasonic experimental set up.

Since a slight ablation occurs very close to the detection point, the plasma is an important source of noise that dominates the backscattered noise from the microstructure. Averaging is then crucial to reduce plasma noise to a lower level. Figure 6 presents the results obtained using a line source configuration and SAFT processing to image the backscattered noise for propagation in the radial direction. The results clearly show noise bands similar to those observed with the immersion technique. No significant difference is observed between the results obtained with the two techniques.

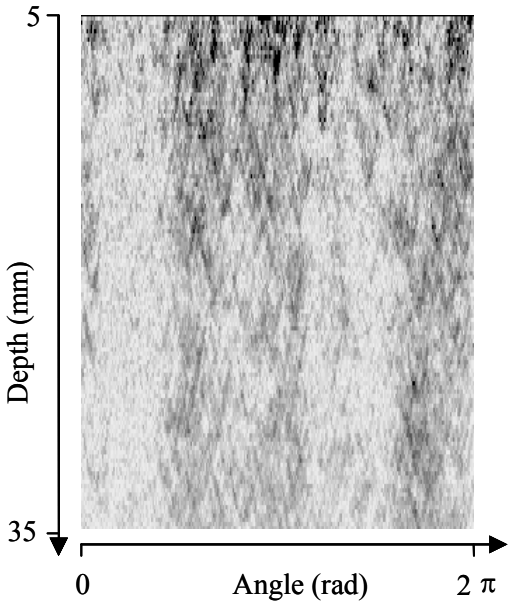

Figure 6. SAFT image of the RMS value of the backscattered noise obtained with a laser line source.

Inspection of a titanium-forged part: A dual phase titanium-forged part has been inspected from its inner surface. The part has a square cross-section with a circular cavity. The experimental set up is illustrated in Figure 7 with the coordinate system (r, θ, z) used. The forged piece is positioned onto a rotating table and the transducer is mounted onto an arm with an acoustic mirror. The angular position θ is related to the rotation of the forged part around its axis. Translating the arm with the acoustic mirror allows scanning along the z-axis. The r-axis corresponds to the radial direction and is equivalent to the time axis of ultrasonic signals for angular scanning (angle θ). It is also obtained directly via the SAFT reconstruction. An unfocused transducer with a 10 MHz center frequency is used. The focusing effect due to the inner curved surface in the plane r-θ is well adapted for performing SAFT reconstruction.

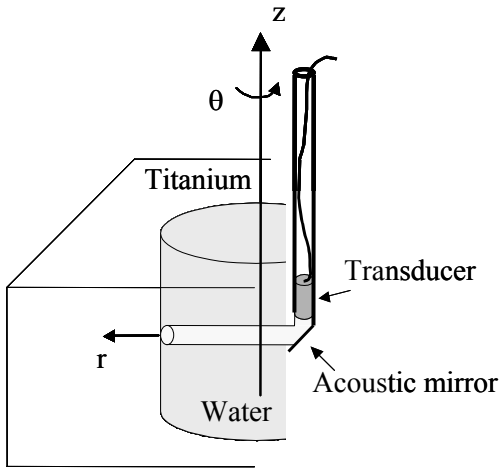

Figure 7. Conventional immersion set up for inspection of the titanium-forged piece from the inner surface.

In Figure 8, a summary of the results obtained for the forged piece is given with the section view and the forging flow lines of the test part. In the figure, the two SAFT images labelled

“interior θ-scan” are obtained for two different z positions. These figures reveal many high-noise regions originating from different locations in the titanium-forged part. The observed high-noise regions are labelled on the section view of the forged part. The region labelled “Noise 4” was observed with axial incident acoustic beam from the bottom of the piece (see “Bottom x-y scan” in Fig. 8). The region labelled “Noise 3” was observed with radial incident acoustic beam from interior θ-scans and from exterior x-scans. Note that the exterior x-scan is obtained with incident acoustic beam from one of the outer flat surface.

For the forged part, the backscattered noise should depend first on the thermo-mechanical process to produce the billet, and then on the forging process to produce the final part. It is expected that the backscattered noise would be affected by the deformation due to the forging since it modifies the shape, orientation and scale of the macrograins. Figure 8 shows the forging flow lines that also provide an indication of the deformation due to forging. In the forged part, the macrograins no longer have columnar shapes elongated along the z-axis since the forging flow lines are functions of both r and z. As a result, the backscattered noise variations observed in the SAFT images are attributable to changes in the macrograin shapes and orientations. The backscattered noise has not only an angular dependence, as in the original billet, but a more complex dependence with r, z and θ. The backscattered noise also depends on the incidence direction of the acoustic beam. Moreover, the effect of the original micro-texture that was observed in the billet could be still present in the backscattered noise of the titanium-forged piece. This effect, along with its angular dependence, should be observed in an area where the macrograins have not been significantly deformed by the forging.

The backscattered noise referred to as “Noise 1”, “Noise 2” and “Noise 4” in Figure 8 does not seem to have angular dependence and comes from areas in the part where the forging has produced important deformations. However, the noise referred to as “Noise 3” comes from an area where the flow lines are almost parallel to the z-axis, similar to the orientation of the macrograins of columnar shape in the original billet. In fact, the SAFT image reveals that the high and low-noise regions possess an angular dependence that could be associated to the original billet. A 3-D representation of this angular dependence is shown in Figure 9 for the RMS values of the backscattered noise averaged along the radial direction, for z-positions between 30 and 55 mm, where “Noise 3” is observed.

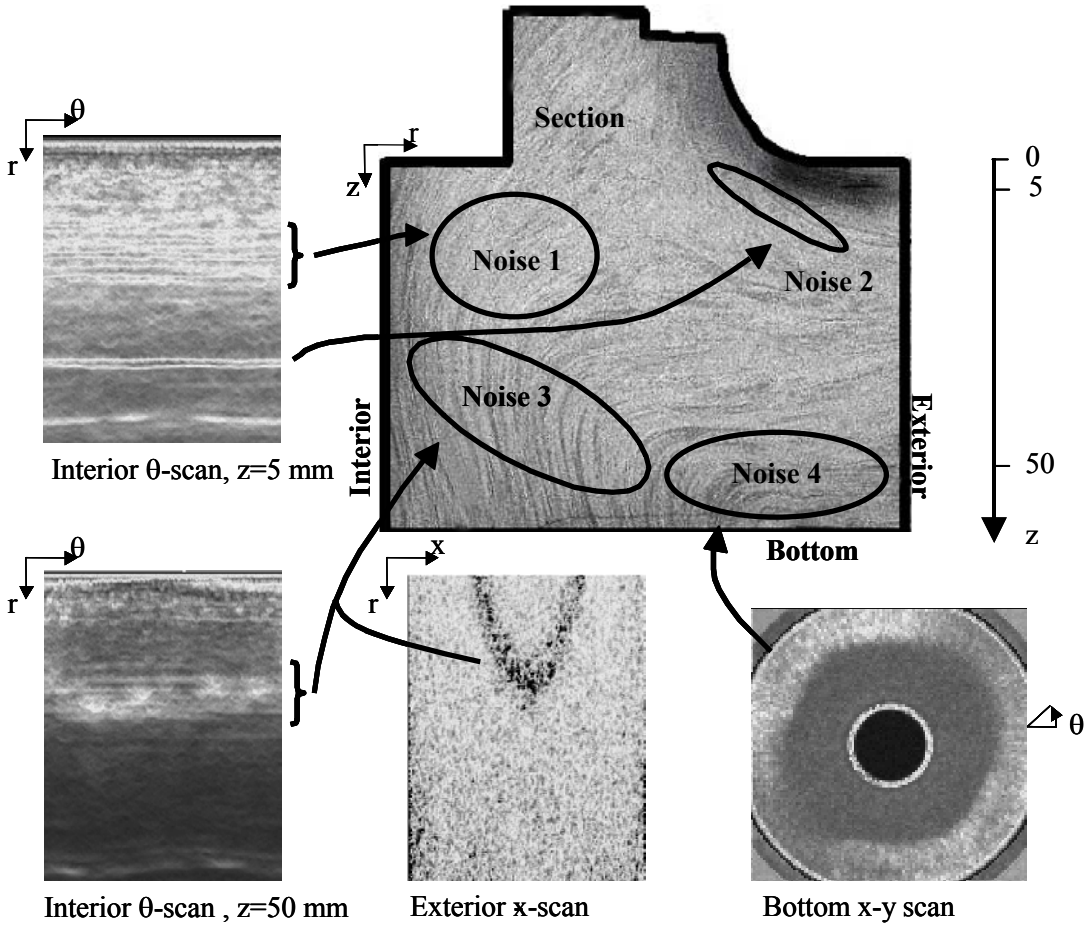

Figure 8. Localization of the sources of backscattered noise and mapping of the forging flow lines.

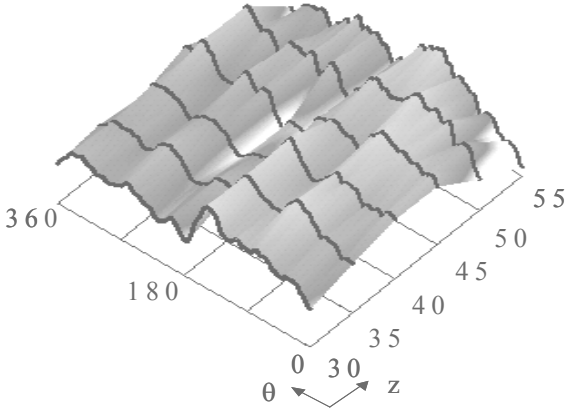

Figure 9. 3-D representation of the RMS value of the backscattered noise around "Noise 3" for z positions between 30 and 55 mm.

Conclusions: A titanium billet and a forged part were tested using ultrasonics to localize highly microtextured regions. Measurements on the billet have provided good results with both the immersion technique and the laser-ultrasonic technique. High and low-noise bands that

correspond to different orientations and texture of the macrograins have been detected and localized. SAFT processing has been used with the two techniques and has shown to improve the contrast of the backscattered noise images.

In the billet, the noise bands are oriented along the radial direction with nearly constant amplitude, independent of the z-position. Measurements on a titanium-forged part have provided more complex images of the backscattered noise since the macrograins have more complex orientations following the forging flow lines. The backscattered noise in the forged part varies with radial direction and z position due to variations of the scattering cross-section. Particular attention has been paid to localize noise regions with angular dependence that could be associated with the original macrograins in the billet. Even if this dependence is expected to be small, a region referred to as "Noise 3" corresponding to a moderate deformation by forging has been found to possess the angular dependence of the billet.

The synthetic aperture focusing technique, presented in this study, for imaging the ultrasonic backscattered noise is well adapted to localize highly microtextured regions in dual phase titanium billets and forged parts.

References:

1 L. Margetan, R. B. Thompson and A. Degtyar, "Survey of ultrasonic properties of aircraft engine titanium forgings", Review of Quantitative Nondestructive Evaluation, Vol. 21, ed. by D. O. Thompson and D. E. Chimenti, pp. 1510-1517, 2002.

2 R. B. Thompson, P. Panetta and F. J. Margetan, "Relationship of the ultrasonic backscattering coefficient of titanium alloys to microtexture", published in 43rd International SAMPE Symposium proceedings, May 31- June 4, pp. 1448-1457, 1998.

3 Y. K. Han and R. B. Thompson, "Ultrasonic backscattering in duplex microstructures: theory and application to titanium alloys", Metallurgical and Materials Transactions A, Vol. 28A, pp. 91-104, 1997.

4 J. H. Rose, "Ultrasonic backscatter from microstucture", Review of Quantitative Nondestructive Evaluation, Vol. 11, ed. by D. O. Thompson and D. E. Chimenti, pp. 1677-1684, 1992.

5 G. Lütjering, "Influence of processing on microstructure and mechanical properties of (α+β) titanium alloys", Materials Science and Engineering, **A243**, pp. 32-45, 1998.

6 K. Y. Han and R. B. Thompson, "Relationship between the two-point correlation of elastic constants and backscattered ultrasonic noise in two-phase titanium alloys", Review of Quantitative Nondestructive Evaluation, Vol. 14, ed. by D. O. Thompson and D. E. Chimenti, pp. 67-74, 1995.

7 A. Blouin, D. Lévesque, C. Néron, F. Enguehard, D. Drolet and J. P. Monchalin, "SAFT processing applied to laser-ultrasonic inspection", Review of Quantitative Nondestructive Evaluation, Vol. 17, ed. by D. O. Thompson and D. E. Chimenti, pp. 611-617, 1998.

8 D. Lévesque, A. Blouin, C. Néron and J. P. Monchalin, "Performance of laser-ultrasonic F-SAFT imaging", Ultrasonics **40**, pp. 1057-1063, 2002.

9 Scruby C. B., Drain L. E. (1990). Laser Ultrasonics, Techniques and Applications. Adam Hilger, New York 1990.

10 J.-P. Monchalin, "Optical Detection of Ultrasound", IEEE Transaction on Ultrasonics, ferroelectrics and frequency control, **33**, pp. 485-499, 1986.